Combust. Sci. and Tech., 180: 45–63, 2008

ISSN: 0010-2202 print/1563-521X online
DOI: 10.1080/00102200701600770

NUMERICAL AND EXPERIMENTAL INVESTIGATION OF BACKDRAFT

Andrej Horvat[1,*], Yehuda Sinai[1], Daniel Gojkovic[2], and Björn Karlsson[3]

[1]*ANSYS Europe Ltd., Abingdon, Oxfordshire, UK*
[2]*Department of Fire Safety Engineering, Lund University, Lund, Sweden*
[3]*Iceland Fire Authority (Brunamálastofnun), Reykjavík, Iceland*

The article describes full-scale backdraft experiments in a shipping container using methane as a fuel. Numerical modelling has followed the experimental setup. The numerical simulations show the initial gravity current, the ignition, the spreading of flame in the enclosure, the external fireball, and the subsequent decay. The Detached Eddy Simulation (DES) approach has been used to model turbulence. In order to describe the combustion process of the mixture from the local ignition to progressive deflagration, three separate combustion models have been implemented for laminar, low- and high-intensity turbulence flow regimes. The calculated ignition time is slightly shorter than the average ignition time observed in the experiments. The fire front progresses through the combustible mixture, generating a cloud of hot gases that are accelerated from the container into the external environment. The velocity increases up to 20 m/s. When the fire front reaches the door, combustion continues outside the enclosure as the fuel has been pushed through the door. The comparison between the calculated time history of relative pressure and the pressure sensor record shows that the numerical simulations slightly overpredict the flame front speed, with a stronger pressure pulse and higher temperatures than the observations.

Keywords: Backdraft; Combustion; Deflagration; Flame; Gravity current

INTRODUCTION

Backdraft is one of the most hazardous events related to under-ventilated fires. Descriptions of this phenomenon may be found in any of the textbooks on fire safety, e.g., Drysdale (1990), or in a variety of papers and reports by Dunn (1988), Fleischmann (1994), Bukowski (1995), Bolliger (1995), Hashigami et al. (1997), Farley et al. (1997), Foster (1997), Fleischmann and McGrattan (1999), Gottuk et al. (1999), Gojkovic (2000) and Foster and Roberts (2003). Briefly, backdraft is caused by fuel vapour being generated after a fire is extinguished, or reduced in intensity by oxygen starvation, and the subsequent introduction of fresh

Received 9 March 2006; accepted 5 June 2007.

The present work was performed as a part of the project "Under-Ventilated Compartments Fires (FIRENET)" (Co. No. HPRN-CT-2002-00197). The project is supported by the EU Research Training Network FP5, which is gratefully acknowledged.

*Address correspondence to andrej.horvat@ansys.com

oxygen, for example by opening of a door. Following the mixing of the fresh air with the fuel rich environment, concentrations can return to the combustible range, and since ignition sources are likely to exist, flaming combustion may be initiated and can develop into a deflagration.

During the past decades fire research has concentrated on the well-ventilated combustion events. Research regarding under-ventilated fire has evolved slower, mainly due to complex physical and chemical processes that occur during this type of event. For this reason, most of research work addressing backdraft has been focused on the initial mixing process between fresh air and combustible gas. Pioneering work on this subject was performed by Fleischmann (1994) and later continued by Fleischmann and McGrattan (1999). The Fire Experimental Unit of the Home Office in England (Foster, 1997) as well as Hokkaido University in Japan (Hashigami et al., 1997) have carried out small-scale backdraft experiments. Notably, in the experimental work done in Japan, natural fuels such as wood were used. However, it is questionable if backdraft did occur during their experiments as the enclosure was opened to the environment over the whole period of the experiment. Regarding situations in which the fire source is uncontrolled, Sinai (1999) reported CFD simulation of an under-ventilated fire generated by a liquid (heptane) pool, accounting for coupling between the fire and the fuel, as well as building leakages, and showed that leakages and wall heat transfer can have a major effect on stratification and the fire dynamics.

Some full-scale experiments of backdraft have also been reported. These include the experiments performed by the University of Canterbury in New Zealand (Bolliger, 1995), and those onboard naval ships using diesel sprays as a fuel source (Farley et al., 1997; Gottuk et al., 1999).

Previous work on theoretical modelling of backdraft has ranged from analytical techniques on the one hand, which are essentially based on lumped-parameter or zonal methodology, to CFD on the other. The modelling examples were published by Fleischmann (1994), Fleischmann and McGrattan (1999), Bukowski (1995) and Weng and Fan (2004). As in the experimental area, most of previous modelling work has only addressed events prior to ignition. There is very substantial amount of literature on gravity currents, which have been the subject of extensive study over many years, in many fields, including the environment. Good examples of that work may be found in the books by Turner (1973) and Simpson (1987). Recently, Yang et al. (2005) reported a successful attempt to simulate an earlier small-scale backdraft experiment performed by Weng et al. (2003), using a laminar flamelet model for partially premixed combustion.

The current article briefly describes experimental work conducted at Lund University, where Gojkovic (2000) performed full-scale experiments of backdraft in a shipping container using methane as a fuel. As backdraft is of particular concern to fire fighters, one of the experiments' objectives was demonstration of backdraft and its explosive power to fire fighters in training. The second objective of the performed experiments was to collect measurements (i.e. temperature, pressure, chemical composition) in order to gain better understanding of the backdraft phenomenon and to provide scientific data for validation of numerical models.

The main objective of this article is to present numerical modelling of backdraft. The simulations include the initial gravity current that is formed after the

door is opened the ignition, spreading of flame in the enclosure, the external fireball, and the subsequent decay. In the present work, the numerical simulations start from the point in time when the door is opened till the backdraft has decayed inside and outside the compartment. The Detached Eddy Simulation (DES) approach (Menter and Kuntz, 2003) was used to model flow's turbulent behaviour. A combustion model, based on the Eddy-Dissipation concept of Magnussen and Hjertager (1976), was developed to describe progressive fire spreading through the mixture of methane, air and combustion products. An additional ignition model was needed to initiate the combustion process when local conditions reach the combustible range for methane.

The simulation results reveal detailed distributions of velocity, temperature and chemical species during backdraft sequence. The article also presents comparisons of calculated pressure and temperature distributions with the experimental data of Gojkovic (2000).

BACKDRAFT EXPERIMENTS

The backdraft experiments were performed as a part of the project "Backdraft and Underventilated Fire," sponsored by the Swedish National Rescue Service Agency. A so-called backdraft container was built to serve as a demonstration device as well as an experimental apparatus. Natural gas has served as fuel during the experiments. A total of 13 experiments were conducted. In 8 cases backdraft did occur following ignition of the mixture with a heated wire. Repeatability of such large scale experiments in a non-uniform environment is always problematic as the ignition and the appearance of subsequent reaction strongly depend on local flow conditions and chemical composition in vicinity of the ignition source as well as on environmental influences (e.g. temperature, wind speed and moisture content). During the experiments, gas temperatures, gas concentrations as well as dynamic and static pressures were measured.

Experimental Setup

The backdraft container (Figure 1) was built from a standard shipping container, which is 5.5 m long, 2.2 m high and 2.2 m wide. The shipping container was modified in several ways to fulfil its purpose as an experimental apparatus.

The container was first sealed and insulated properly in order to keep the heat and the unburnt gases in the container. It was not absolutely air-tight, so several leakages may have existed mainly around the pressure relief panel. The container's walls were insulated with fibreglass insulation and the floor was covered with concrete. A pressure relief panel was placed on one of the short ends of the container. Its function was to vent any unwanted pressure buildup that might occur during the experiments in order to protect the construction from severe damage. To allow better visualisation of the backdraft during demonstrations, a window with fire-rated glass that withstands high temperature and pressure changes was installed in the container. An opening was made at the other short side of the container to control the introduction of air into the container. The opening was 0.8 m high and covered the whole width of the container. It was placed at mid-height of the container.

Figure 1 Backdraft container.

The opening was covered by a hatch that can be opened by pulling a wire from a safe distance. A roof protected the container from precipitation.

In addition to the modifications to the container mentioned above, a few smaller instalments were made in the container. A gas burner is situated on the floor at the rear end (near the pressure relief panel) of the container centreline as shown in Figure 2. The burner measures $0.3\,\mathrm{m} \times 0.3\,\mathrm{m}$ and it is filled with sand. A hole in the concrete floor allows gaseous fuel to enter the burner. An electrical spark igniter is placed at the edge of the burner to start initial methane combustion. To be able to trigger backdraft in the container, an electrically heated metal wire was used as an

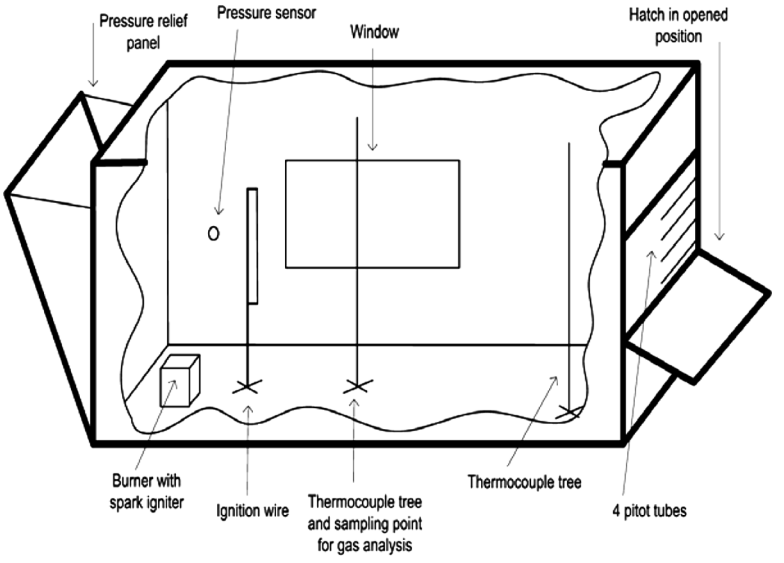

Figure 2 Sketch of measuring equipment in the backdraft container.

ignition source (Figure 2). The wire is approximately 1 m long and is vertically oriented. It can also be moved vertically.

To evaluate the experiments in a quantitative and a qualitative way, pressure, temperature and gas inflow were measured during the experiments. To measure temperature, two thermocouple trees (TCT) were positioned in the container. Each TCT contains 5 thermocouples, separated by a distance of 0.4 m. The topmost thermocouple was positioned 20 cm under the ceiling. During some of the experiments 3 additional thermocouples were placed on the wall opposite the window. In order to calculate flow's dynamic pressure in the opening, fluid density needs to be obtained. Therefore, 3 thermocouples were also placed in vertical direction across the opening. All mentioned thermocouples were type K and 0.25 mm thick.

A piezo-resistive pressure sensor was installed in the container. The purpose of this pressure sensor is to track the static pressure build-up. The sensor measures the pressure in the container during the whole experiment. When the pressure buildup reaches a pre-determined trigger-value, the sensor is triggered and the pressure history is recorded for a total of 6 s. Most of the measurements made with the pressure sensor were unsuccessful. The trigger level must be set quite low (70 Pa) for the sensor to be triggered. When the hatch opens, the vibration caused by the falling hatch is strong enough to trigger the sensor. The 3 bi-directional pitot tubes were placed in the opening to record changes in dynamic pressure. On each of the tubes a thermocouple was placed. Knowing pressure and temperature (density) of the flowing gas, velocity of the gas can be calculated. Since the tubes are bi-directional, the direction of the gas-flow is also given.

The main parameter that determines the outcome of a possible backdraft situation is the amount of combustible gases in the enclosure. In the experiments natural gas was used as a fuel. Using a gaseous fuel eases the control of the amount of gas that enters the container. Three different methods were applied to measure the amount of fuel in the container. The pressure level in the tank originally containing natural gas was recorded, as the pressure change in the tank corresponds to the amount of gas that entered the container. Also, the tank was placed on a scale and the mass loss rate was calculated. The third method involved a Dräger Multiwarn II gas instrument, which is equipped with one infrared sensor for measuring methane concentration, and with 2 electrochemical sensors for measuring carbon dioxide and oxygen concentrations.

Experimental Procedure

The purpose of the experiments was to simulate a real backdraft scenario using natural gas. In reality, backdraft most often occurs due to pyrolysis of solid fuel. However, natural gas has a lot of similarities with gaseous products of pyrolysis such as a density lower than air and flammability within certain limits. Beside that, it is much harder to control the amount of gaseous fuel produced by pyrolysis of a solid fuel than to measure the release of natural gas into the container.

The experiment starts by closing the hatch and the pressure relief panel. At this stage the container is rather air-tight. A small ventilation hole is opened and the spark igniter located at the burner ignites the gas. The burner produces a 2 m high

Figure 3 Fireball in the experiment No. 4.

flame with heat release rate of approximately 600 kW. When the flame is stabilised, the small ventilation hole is covered by a hatch. The reason for opening the ventilation hole is to vent the overpressure created when igniting the flame. Due to oxygen vitiation, the flame dies out after approximately 1 min.

Even after the flame has gone out, the natural gas is kept flowing through the burner into the container. This procedure simulates the pyrolysis process when a high concentration of combustible gas is generated. When the desired fuel concentration is reached, the gas flow is turned off. If no combustion was present in the container, the fuel release would amount to 25% of the whole container volume. The hatch that covers the slot opening is then opened and fresh air is allowed to enter the container. The ignition source is turned on. The air mixes with the natural gas creating a flammable region. When the flammable region reaches the ignition source, the gas mixture is ignited. The temperature rises very quickly causing a volumetric expansion that expels unburnt gases outside the container. The flame propagates across the container. Finally, the unburnt gases outside the container are combusted in a dramatic fireball as shown in Figure 3.

From 13 experiments that were performed only in 8 cases the ignition wire managed to trigger sustainable deflagration. The ignition threshold of a combustible mixture strongly depends on concentration and temperature, and it is still a subject of intensive research. In a dynamic environment, local flow conditions also have a significant effect. To the authors' opinion, poor repeatability of backdraft occurrence is associated with a weak ignition source. This means the ignition threshold of the mixture close to the ignition wire is too high in comparison to the energy of the heated wire. Also, it needs to be emphasized that it is extremely hard to get reliable measurements from such experiments. This is mainly due to two different time-scales of the backdraft phenomena. Namely, initial heating of the container and accumulation of the combustible gas is happening on much longer time scale than subsequent gravity current of entering fresh air and the ignition of the mixture.

NUMERICAL MODEL

The CFD model closely followed the experimental setup of Gojkovic (2000). As in the experiments, methane was used as a fuel. The following single step chemical reaction shows conversion of chemical species:

$$CH_4 + 2\left(O_2 + \frac{0.79}{0.21}N_2\right) \Rightarrow CO_2 + 2H_2O + 2\frac{0.79}{0.21}N_2 \qquad (1)$$

The simulations were performed using CFX-5.7.1 software. To achieve realistic backdraft simulations, additional mathematical models were added to those already available in the standard version of the code. The details will be given later. The transient model starts at the instant at which the door opens and fresh air enters the compartment.

Geometrical Considerations and Initial Assumptions

The geometry of the model is shown in Figure 4. It is a 1:1 scale of the experimental apparatus. The enclosure is positioned in the left half of the simulation domain, which is 22 m long, 10 m deep and 10 m wide. The enclosure is also lifted for 40 cm above the ground. A roof plate is positioned nominally 70 cm above the enclosure and is inclined at 5° from the horizontal position. The roof was included in the model because of its potential ability to influence the mixing at the door, as well as external dispersion of the combustible mixture and hence the external fireball.

Initially, the container is filled with a mixture that contains methane, air and combustion products. The spatial distribution of the various species was inhomogeneous but unmeasured. Gojkovic (2000) reported the total amount of methane that was released into the compartment. Although, the amount was partially reduced due to initial burning, the resulting composition of the mixture was rich in unburned methane and combustion products with a relatively small amount of oxygen that was unable to support burning. In view of the uncertainties, the following initial content of methane and carbon-dioxide was assumed in the model:

$$\overline{\Psi}_{CH_4} = 0.22, \quad \overline{\Psi}_{CO_2} = 0.02 \tag{2}$$

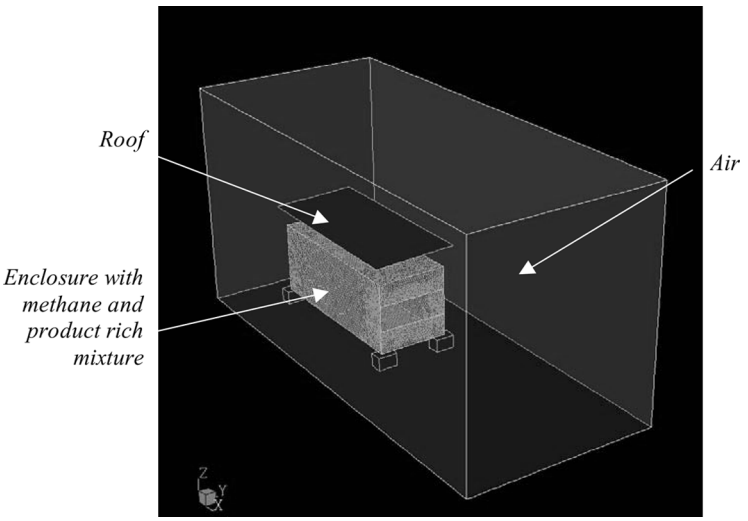

Figure 4 Geometrical arrangement of the backdraft model.

The rest of the mixture composition can be determined from the reaction equation (1):

$$\overline{\Psi}_{H_2O} = 0.04,\ \overline{\Psi}_{O_2} = 0.1196,\ \overline{\Psi}_{N_2} = 0.6004 \tag{3}$$

The initial velocity was set to 0.0. Some thermal data was available, and a linear vertical temperature profile was prescribed inside the enclosure:

$$T_{in} = \frac{98^\circ\mathrm{C} - 62^\circ\mathrm{C}}{1.6\,\mathrm{m}}(z + 0.7\,\mathrm{m}) + 62^\circ\mathrm{C} \tag{4}$$

as measured in the experimental case No. 9 after 420 s (Gojkovic, 2000).
For the external initial composition, we assumed fresh air:

$$\overline{\Psi}_{CH_4} = 0.0,\ \overline{\Psi}_{O_2} = 0.21,\ \overline{\Psi}_{N_2} = 0.79,\ \overline{\Psi}_{CO_2} = 0.0,\ \overline{\Psi}_{H_2O} = 0.0 \tag{5}$$

and an initial temperature of 5°C.

For the simulations' boundary conditions, the no-slip, smooth, adiabatic boundary conditions were set for all walls. At the outermost boundaries of the domain, wall conditions were set at the floor and pressure conditions (openings) at the remaining boundaries, with an ambient temperature of 5°C. At openings, flow may enter or leave, depending on the local pressure distribution at the boundary.

Modelling Approach

Due to turbulence and changes in material composition, the Favre-averaged form of transport equations have to be used. The full set of mass and momentum transport equations can be found in any classical fluid dynamics book (e.g., Bird et al., 1960) and therefore will not be repeated here. Beside the mass and the momentum transport equation for the mixture, the transport equations for the components CH_4, O_2, H_2O and CO_2 are also needed:

$$\partial_t(\rho\bar{\xi}_c) + \partial_j(\rho\bar{v}_j\bar{\xi}_c) = \partial_j(\rho D_c\partial_j\bar{\xi}_c) + \overline{S}_c - \partial_j(\rho\overline{v'_j\xi'_c}) \tag{6}$$

where S_c is a source term due to the chemical reaction involving component c. Furthermore, the energy equation has to be written for the total specific enthalpy:

$$\partial_t(\rho\bar{h}_{tot}) - \partial_t p + \partial_j(\rho\bar{v}_j\bar{h}_{tot}) = \partial_j(\lambda\partial_j\overline{T}) + \sum_n \vartheta_n\overline{S}_c - \partial_j(\rho\overline{v'_j h'_{tot}}) \tag{7}$$

In the present work, a Detached Eddy Simulation (DES) model (Menter and Kuntz, 2003) was used to model turbulence. Using the Large Eddy Simulation (LES) turbulence model to resolve flow structures in wall boundary layer flows at high Re numbers is extremely expensive and therefore not useful for most industrial flow simulations. The DES model is an attempt to combine elements of the RANS and the LES approach into a hybrid formulation, where the Shear Stress Transport (SST) model is used inside attached and mildly separated boundary layers, and the LES model is applied in massively separated regions.

To distinguish these two regions, a turbulence length scale, calculated as

$$l_{RANS} = \frac{\sqrt{k}}{C_\mu \omega} \tag{8}$$

is compared with a length scale associated with the local grid spacing Δ in the LES model:

$$l_{LES} = C_{DES}\Delta \tag{9}$$

The DES model switches from the SST model to the LES model in the regions where the turbulence length scale l_{RANS} is larger than the local LES model scale l_{LES}.

The turbulence kinetic energy is calculated as

$$\partial_t(\rho k) + \partial_j(\rho \bar{v}_j k) = \partial_j\left(\left(\mu + \frac{\mu_t}{\sigma_{k3}}\right)\partial_j k\right) + \widetilde{P} - F_{DES} C_\mu \rho \omega k \tag{10}$$

where F_{DES} is a blending function:

$$F_{DES} = max\left(\frac{l_{RANS}}{l_{LES}}(1 - F_2), 1\right) \tag{11}$$

which switches between the RANS and the LES model scale. Turbulence eddy frequency ω is calculated with the following transport equation:

$$\partial_t(\rho\omega) + \partial_j(\rho \bar{v}_j \omega) = \alpha_3 \rho S^2 + \partial_j\left(\left(\mu + \frac{\mu_t}{\sigma_{\omega 3}}\right)\partial_j \omega\right) + (1 - F_1)\frac{2\rho}{\sigma_{\omega 2}}\partial_j k \partial_j \omega - \beta_3 \rho \omega^2 \tag{12}$$

Turbulent viscosity is defined as in the SST model:

$$\mu_t = \frac{a_1 k}{\max(a_1 \omega, F_2 S)} \tag{13}$$

and turbulence heat and mass fluxes are calculated as

$$\rho\overline{v_j' h_{tot}'} = -\frac{\mu_t}{Pr_t}\partial_j \bar{h} \quad \text{and} \quad \rho\overline{v_j' \xi'} = -\frac{\mu_t}{Sc_t}\partial_j \bar{\xi} \tag{14}$$

Usually the molecular mass diffusivity ρD is small in comparison to the turbulence mass diffusivity μ_t/Sc_t and often unknown. Note that the parameters σ_{k3}, α_3, $\sigma_{\omega 3}$, β_3 and F_2 are not constants. Their values are calculated locally during the simulations as in the SST model (Menter and Kuntz, 2003). Sensitivity analysis of the turbulence model parameters is beyond the scope of the present article.

Modelling of combustion was based on the eddy-dissipation concept, where the combustion reactions are lumped together in a one step reaction, which is fast relative to the transport processes in the flow. In order to describe the combustion process of the mixture from the local ignition to progressive deflagration, three separate

combustion models were used for laminar, low- and high-intensity turbulence flow regimes.

In the laminar regime, the reaction rate of fuel is approximated with a relation using a constant burning speed U_B and the molecular concentration of fuel $\bar{\zeta}_f$:

$$R_{f,Lam} = -\frac{U_B}{V^{1/3}}\bar{\zeta}_f \tag{15}$$

For methane, the burning speed $U_B = 0.36\,\mathrm{m/s}$ was taken from Drysdale (1990). After the transition to turbulence the flame front becomes distorted due to turbulence eddies. For the low-intensity turbulence regime, Schelkin approximated the increase in flame front area with conical structures (Figure 5) as described by Kuo (1986).

The increased flame front area can be approximated with $A_c = A_B(1 + 4(h/l')^2)^{1/2}$. As the height of the conical structures is related to turbulence fluctuations $h = u_{rms}l'/U_B$, the final expression for the fuel reaction rate is:

$$R_{f,Low} = -\frac{U_B}{V^{1/3}}\left(1 + \frac{8}{3}(k/U_B^2)\right)^{1/2}\bar{\zeta}_f \tag{16}$$

The eddy-dissipation model (Magnussen and Hjertager, 1976) describes combustion in the high-intensity turbulence regime. The reaction rate depends on the flow timescale $t_{flow} = k/\varepsilon$ and the molecular concentrations of fuel, oxidizer and products. Due to the product rich environment, the product dependence of the reaction rate was left out from the model. Thus, the reaction rate of the fuel is defined as:

$$R_{f,High} = -C_A\frac{\varepsilon}{k}min\left(\bar{\zeta}_f, \frac{\zeta_{o_x}}{s}\right) \tag{17}$$

where the coefficient C_A was set to 8.0.

In the performed simulations, higher of the both reaction rates (16) and (17) was taken in each timestep using the expression:

$$R_f = -max\left(\frac{U_B}{V^{1/3}}\left(1 + \frac{8}{3}(k/U_B^2)\right)^{1/2}, C_A\frac{\varepsilon}{k}\right)min\left(\bar{\zeta}_f, \frac{\bar{\zeta}_{o_x}}{s}\right) \tag{18}$$

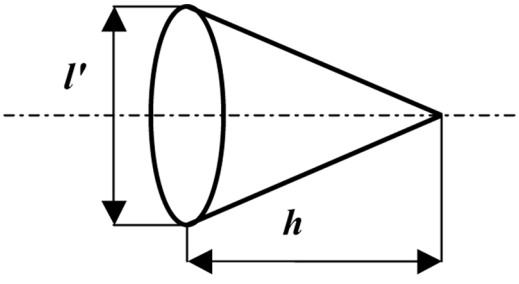

Figure 5 Enhancing of flame surface due to turbulence (Kuo, 1986).

The combustion reaction rate is further limited by multiplying (18) with an extinction temperature function F_{ext}, which was defined as a linear function between temperatures T_{lim} and T_{auto}:

$$F_{ext} = min\left(max\left(\frac{T - T_{lim}}{T_{auto} - T_{lim}}, 0\right), 1\right) \tag{19}$$

The function F_{ext} does not allow combustion before T_{lim} is exceeded. This ensures that fire starts only when the ignition model raises the temperature above T_{lim}. On the other hand, the function F_{ext} allows only limited combustion before the auto-ignition temperature T_{auto} is reached. In the presented simulations T_{lim} and T_{auto} were set to 400 K and 900 K, respectively. This gives a rough approximation of flammability diagrams that are found in Drysdale (1990) or published by N.V. Nederlandse Gasunie (1988).

The ignition of mixture that occurs as an integral part of the numerical simulation required special attention. It is achieved with a heat source of the cumulative specific energy $I_{ign} = 1\,\mathrm{J/cm^3}$. The heat source is triggered when the mixture is inside the flammability limits anywhere along the position of the ignition wire (Gojkovic, 2000). The ignition model is triggered at the wire location as soon as the ignition criterion is satisfied.

The needed strength of the ignition source I_{ign} was determined using measured data from Bosch (1976) for fuel rich mixtures. In order to predict the time of the ignition realistically, the whole flammability diagram (Drysdale, 1990) was examined at each timestep. The ignition heat source is distributed over $\Delta t_{ign} = 0.02\,\mathrm{s}$ (or 20 timesteps) in the form of an even function:

$$\dot{I}_{ign} = \sin^2(\pi(t - t_{ign})/\Delta t_{ign})\frac{2I_{ign}}{\Delta t_{ign}} \tag{20}$$

The duration of the ignition phase is significantly longer in comparison to the spark-ignition in an internal combustion engine, where the ignition phase of the stoichiometric mixture is approximately 1 ms (Heywood, 1988).

RESULTS AND DISCUSSION

Three-dimensional numerical mesh with 162,552 grid nodes was generated to perform the analysis. The mesh consisted of tetrahedra and prisms; the latter are aligned with walls to improve resolution of the boundary layer structure. The average mesh spacing inside the enclosure was 5 cm. In addition, the mesh was further refined around the ignition source and the container entrance. As numerical results can be grid dependent, special care was taken to construct numerical grids with sufficient resolution and uniformity. Parallel computation took approximately 15 days on 4 processors with 3 GHz processor speed.

The initial timestep was set to $\Delta t = 0.02\,\mathrm{s}$ taking into account the timescale $L/\sqrt{\beta g h}$ of the initial gravity wave behaviour. In the experiments (Gojkovic, 2000) the ignition was achieved with a hot wire. In the numerical model, methane and

oxygen concentrations were checked in a small cylindrical volume at the back of the enclosure, 1.3 m from the wall, at each timestep. If the methane concentration was locally within its varying flammability range, a thermal energy source (20) was imposed over the time interval $\Delta t_{ign} = 0.02$ s. After ignition was reached, the time step was reduced to $\Delta t = 0.001$ s. Figure 6 shows a fireball that is progressing outside the container due external combustion of expelled unburnt gases.

From the simulation results, instantaneous fields of velocity, pressure, temperature and mass fractions were obtained. Figure 7 shows the instantaneous fields before the ignition ($t = 10.0$ s), during occurrence of a gravity wave. The stream of fresh and cold air enters the enclosure and moves along the bottom toward the back wall. It can be identified as a high velocity region (Figure 7a) with low temperature (Figure 7b) and low mass fraction of methane (Figure 7c). As it reflects from the back wall, a large premixed region is created, where the mixture is within the flammability limits.

The time of ignition was compared with the experimental data of Gojkovic (2000) and presented in Table 1. The ignition point was reached at $t_{ign} = 14.6$ s. The calculated ignition time is slightly shorter than the average ignition time observed in the experiments. The difference may be due to different identification of the ignition event. In the experiments, the ignition time is determined by visual identification of fire, whereas in the numerical calculation, the ignition time is defined by the flammability limits being reached around the ignition wire and the start of the ignition algorithm. Also, the energy in the ignition source used in the experiments might not be high enough to instantly ignite the gases, even if they are within the flammable region.

Figure 8 shows the instantaneous fields of velocity, temperature and mass fractions of methane well after the ignition ($t = 14.6$ s). At this stage, the flame front has propagated over the upper half of the container (Figure 8b). The fire front progresses through the combustible mixture generating a cloud of hot gases that is moving upwards due to buoyancy. As the hot gases expand, the flow is accelerated from the container to the external environment. The velocity increases up to 20 m/s

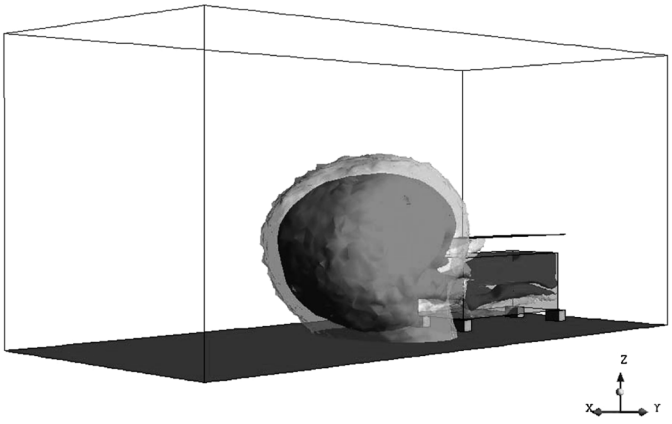

Figure 6 Temperature isosurfaces of 400 K and 900 K, t = 16.7 s.

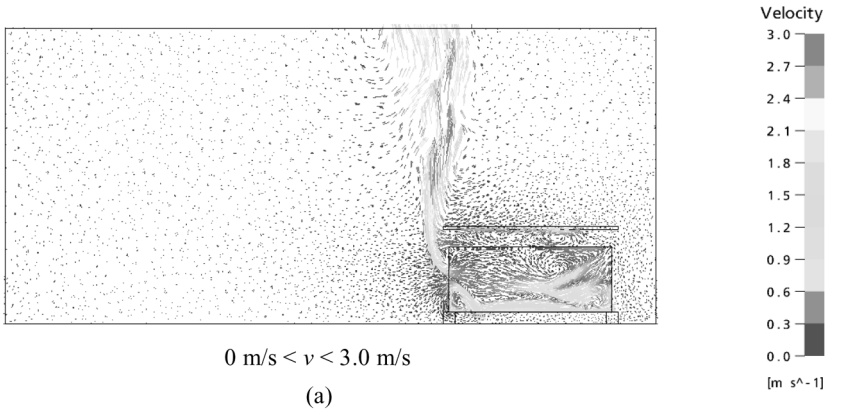

0 m/s < v < 3.0 m/s

(a)

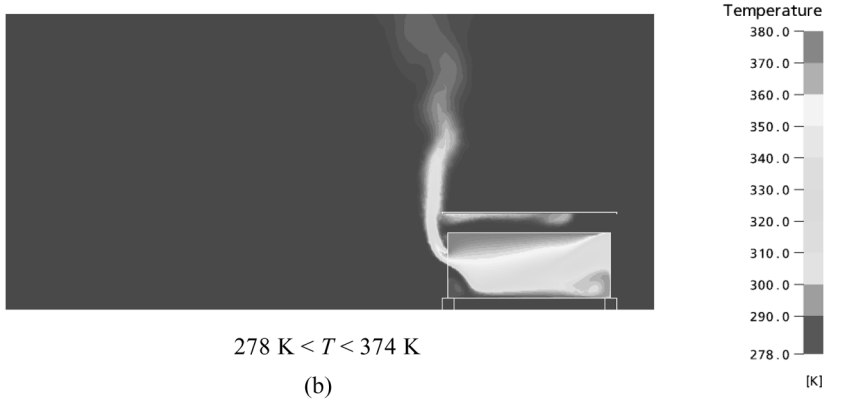

278 K < T < 374 K

(b)

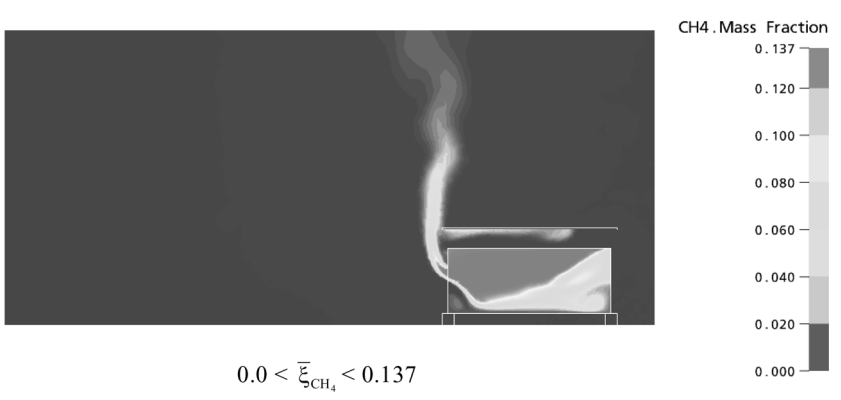

$0.0 < \overline{\xi}_{CH_4} < 0.137$

(c)

Figure 7 Velocity (a), temperature (b) and methane mass fraction (c) before the ignition, t = 10.0 s, y = 0.0 m cross-section view.

(Figure 8a). Mass fraction of methane rapidly decreases in the area of the fire, which creates a methane depleted region in the middle of the container (Figure 8c). Some of the fuel is also pushed out of the enclosure.

Table 1 Comparison of the time to ignition; the experimental data for methane concentration in the enclosure are calculated from supply vessel weight measurements (Gojkovic, 2000)

	$\overline{\Psi}_{CH_4}$	t_{ign} [s]
Experiment no. 4	0.35	35
Experiment no. 7	0.28	46
Experiment no. 9	0.31	25
Experiment no. 10	0.27	15
Experiment no. 11	0.20	32
Experiment no. 12	0.27	34
Experiment no. 13	0.23	22
Numerical simulation	0.24	14.6

Figure 9 shows the instantaneous fields of velocity, temperature and mass fractions of methane where the fire front already propagates outside the enclosure ($t = 16.8$ s). When the fire front reaches the door, combustion continues outside the enclosure (Figure 9b) as the fuel has been pushed through the door. The external combustion further accelerates expelled gases, which form a horizontally elongated cloud. As the gases are much hotter than surroundings, they slowly raise and eventually disappear from the simulation domain. In the container, the temperature starts to decrease due to the consumed methane and consequently its low mass fraction (Figure 9c).

Time distributions of relative pressure (p-p_{amb}) and temperature after the ignition were also compared with the measured values of Gojkovic (2000). Unfortunately, the time interval between temperature measurements is too long for reliable comparison of results. Nevertheless, some conclusions can be obtained from the currently available sets of data.

Figure 10 shows comparison between the calculated time distribution of relative pressure and a record taken from the pressure sensor (Figure 2). The present combustion model is simple and computationally very efficient. Unfortunately, it only barely takes into account the reaction kinetics, which depends on local and temporal chemical composition and temperature. As a consequence, the total amount of consumed fuel is larger than seen in the experiments. This lead to a slightly stronger pressure pulse (Figure 10) and higher temperatures (Figure 11).

CONCLUSIONS

As a part of an experimental program, eight successful full-scale backdraft experiments were performed at Lund University. The experimental apparatus was built from a standard shipping container, which was appropriately modified. Natural gas, which was used as a fuel, was pumped into the sealed and insulated container to produce a fuel and product rich mixture where burning is unsustainable due to lack of oxygen. Fresh air was introduced through a horizontal opening to dilute the mixture and return concentrations to the combustible range. The backdraft was initiated with a heated wire at the back of the container, which triggered the backdraft when conditions local to the wire reached the flammable range. A flame

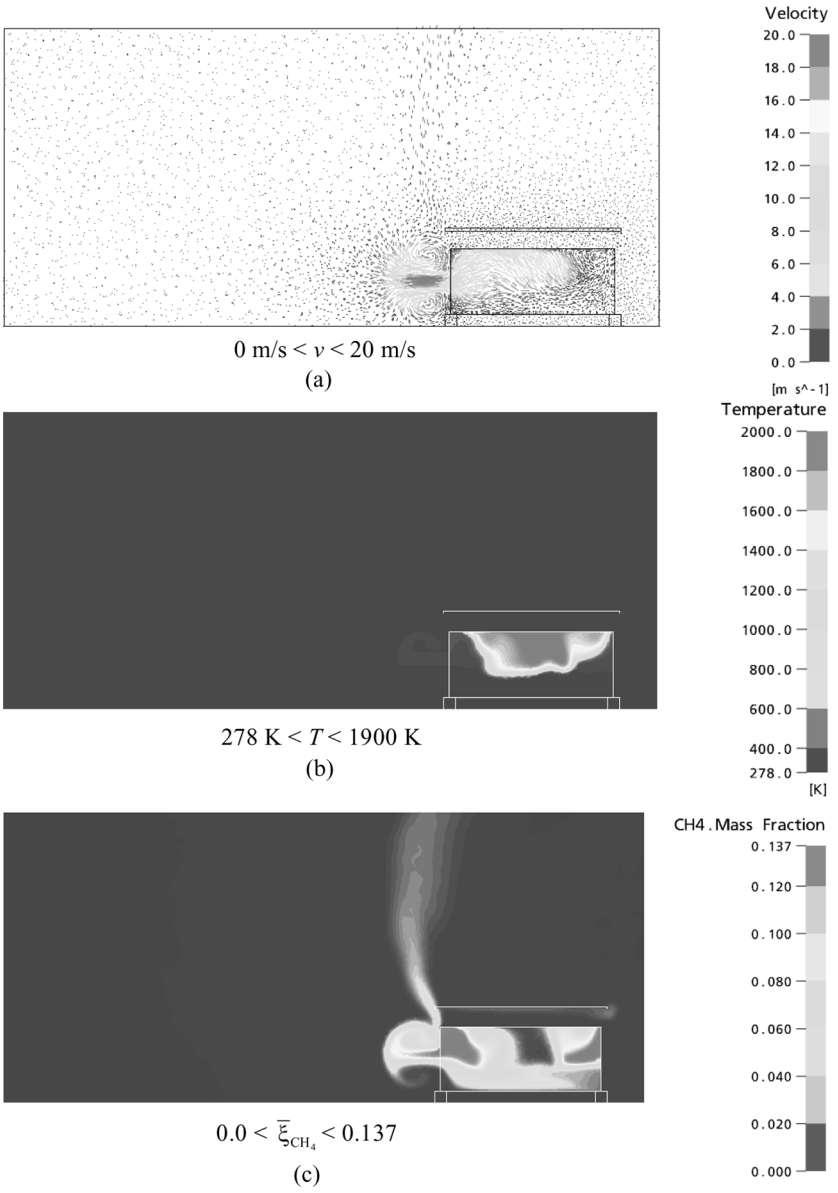

Figure 8 Velocity (a), temperature (b) and methane mass fraction (c) after the ignition, t = 15.9 s, y = 0.0 m cross-section view.

front propagated across the container and formed an external fireball. During the experiments, pressure, temperature and gas inflow were measured.

For prediction of the backdraft phenomena, a CFD model was built and numerical simulations of one of the full-scale backdraft experiments were conducted to verify modelling assumptions. The mathematical model describes the system from the time at which the enclosure door was opened. Thus, the inert gravity current,

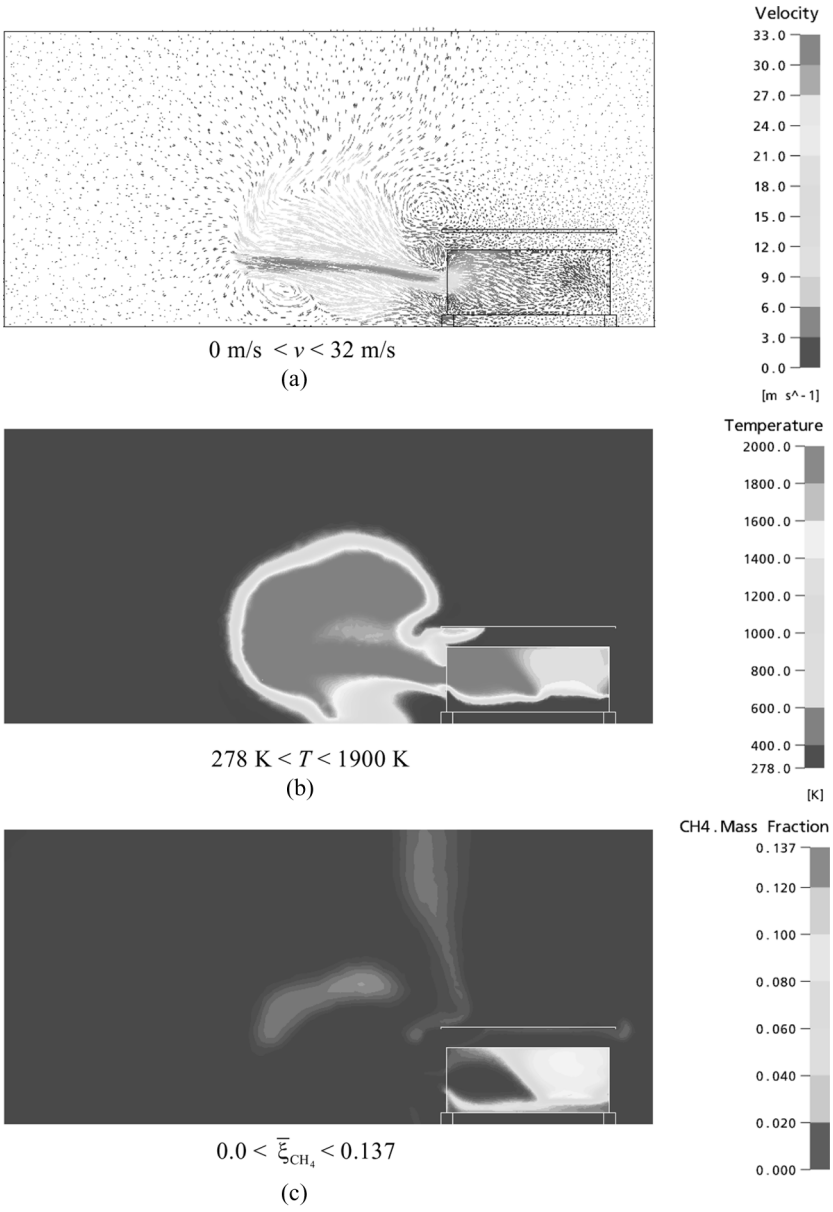

Figure 9 Velocity (a), temperature (b) and methane mass fraction (c) after the ignition, t = 16.8 s, y = 0.0 m cross-section view.

which precedes the backdraft, was computed as part of the simulation. The DES turbulence model was used to model turbulence behaviour. The ignition model, which has been developed, initiated the combustion process when conditions at any part of the heated wire in the rig reached concentrations, which lay within the

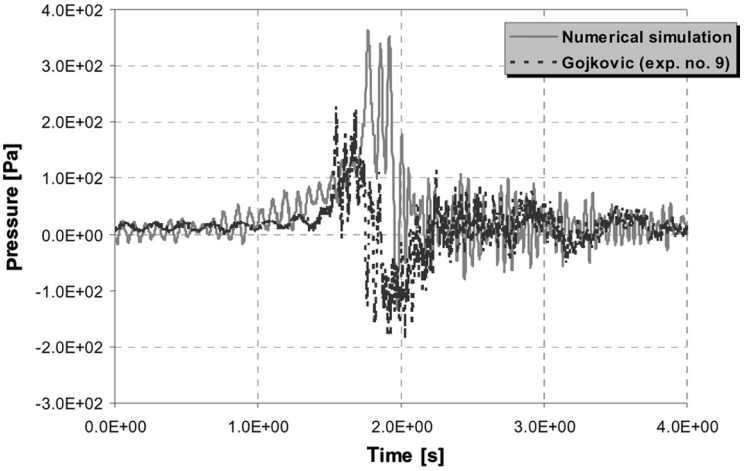

Figure 10 Time distribution of relative pressure after the ignition.

flammable range. To describe combustion in fuel- and product-rich environments, a customised combustion model was constructed from three separate combustion models.

The numerical simulations predicted ignition after 14.6 seconds, which is slightly shorter than in the experiments. The difference was probably due to different identification of the ignition event between the experimental observation and the mathematical definition in the simulations. The simulations also predicted a propagating flame front, which generates local flows with velocities up to about 30 m/s near the door. As in the experiments, the analysis demonstrated that burning occurs not only inside the compartment, but also outside. This is caused by the expulsion of

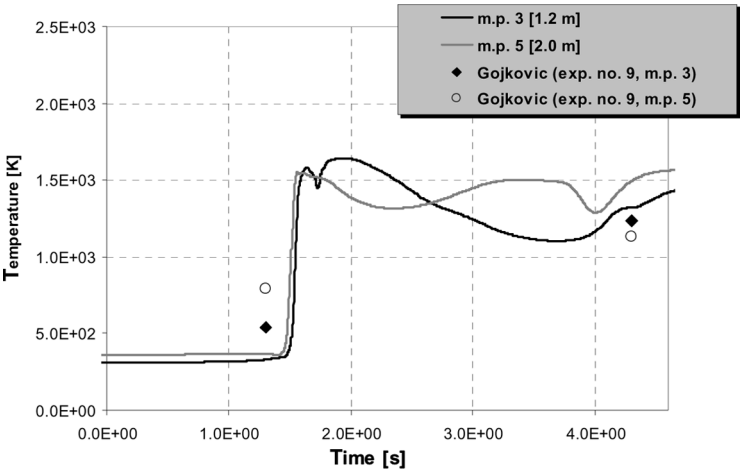

Figure 11 Time distribution of temperature after the ignition.

fuel gas from the compartment upstream of the primary flame front. Differences between the simulations and the experimental data are greater for pressure and especially for temperature. This is probably attributable to the shortcomings in the combustion models, which overpredict the reaction rate. Nevertheless, it should be noted that the experiments were not always repeatable, and in some nominally identical situations, backdraft was observed in one test but not another. The simulations and the comparison with the experimental results reported here are encouraging. Nevertheless, there is clearly a need for improving the quality of the results.

NOMENCLATURE

Latin

A_B, A_c	surface of a flame front
C_A, C_B	Eddy-Dissipation model constants
C_{DES}	$=0.61$, constant
C_μ	$=0.09$, constant
D	molecular diffusivity
F_2, F_{DES}	turbulence model blending functions
F_{ext}	extinction function
g	gravity acceleration
H	Heaviside unit step function
h	height of the container
$\bar{h}_{tot}$	$= c_p\overline{T} + 0.5\rho\bar{v}_j\bar{v}_j$, total specific enthalpy
I_{ign}	specific energy of ignition
k	turbulence kinetic energy
L	length of the container
l	length scale
P	turbulence production term
Pr	Prandtl number
p, p_{amb}	pressure, ambient pressure
R	reaction rate
S	source term, invariant measure of the strain rate
Sc	Schmidt number
s	stoichiometric ratio
T	temperature
t	time scale
U_B	flame speed
u_{rms}	turbulence intensity
V	volume of finite computational cell
v	velocity
x, y, z	spatial coordinates

Greek Letters

β	$(\rho_{air}/\rho_{mixture}) - 1$
Δ	local grid spacing
ε	turbulence dissipation rate
ζ	molar concentration
ϑ	heat of combustion
λ	thermal conductivity
μ, μ_t	dynamic viscosity, eddy dynamic viscosity
ξ	mass fraction
ρ	density
ψ	volume/molar fraction
ω	turbulence frequency

REFERENCES

Bird, R.B., Stewart, W.E., and Lightfoot, E.N. (1960) *Transport Phenomena*, Wiley, New York, USA.

Bolliger, I.J. (1995) *Full Residental-Scale Backdraft*, University of Canterbury, New Zealand.

Bosch, R. (1976) *Automotive Handbook*, Robert Bosch GmbH, Stuttgart, Germany.

Bukowski, R.W. (1995) Modelling backdraft: The fire at 62 Watts Street. *NFPA J.*, **89**, 85–89.

Drysdale, D. (1990) *An Introduction to Fire Dynamics*, John Wiley & Sons, Chichester, UK.

Dunn, V. (1988) Beating the backdraft. *Fire Eng. J.*, **14**, 44–48.

Farley, J.P., Gottuk, D.T., and Williams, F.W. (1997) *The Development and Mitigation of Backdrafts: A Full-Scale Experimental Study*, Naval Research Laboratory, Washington, USA.

Fleischmann, C.M. (1994) *Backdraft Phenomena*, NIST-GCR-94-646, NIST, Gaithersburg, USA.

Fleischmann, C.M. and McGrattan, K.B. (1999) Numerical and experimental gravity currents related to backdrafts. *Fire Safety J.*, **33**, 21–34.

Foster, J.A. (1997) The fire experimental unit's backdraught simulator. *Fire Res. News*, **21**, 36–38.

Foster, J.A. and Roberts, G.V. (2003) *An Experimental Investigation of Backdraft*. Fire Research Division, ODPM, London, UK.

Gojkovic, D. (2000) *Initial Backdraft Experiments*, Report 3121, Department of Fire Safety Engineering, Lund University, Sweden.

Gottuk, D.T., Peatross, M.J., Farley, J.P., and Williams, F.W. (1999) The development and mitigation of backdraft: A real-scale shipboard study. *Fire Safety J.*, **33**, 261–282.

Heywood, J.B. (1988) *Internal Combustion Engine Fundamentals*, McGraw-Hill, NewYork, USA.

Hashigami, T., Hayasaka, H., Ito, J., Kojima, H., Kodou, Y., and Ueda, T. (1997) *Backdraft Experiments in a Small Compartment*, Hokkaido University, Sapporo, Japan.

Kuo, K.K. (1986) *Principles of Combustion*, John Wiley and Sons, New York.

Magnussen, B.F. and Hjertager, B.H. (1976) On mathematical modeling of turbulent combustion with special emphasis on soot formation and combustion. *Proc. Combust. Instit.*, **16**, 719–729.

Menter, F.R. and Kuntz, M. (2003) *Development and Application of a Zonal DES Turbulence Model for CFX-5*, CFX-Validation Report, CFX-VAL17/0503.

N.V. Nederlandse Gasunie (1988) *Physical Properties of Natural Gases*, Groningen, Netherlands.

Simpson, J.E. (1987) *Gravity Currents in the Environment and the Laboratory*, Wiley, New York.

Sinai, Y.L. (1999) Comments on the role of leakages in field modelling of under-ventilated compartment fires. *Fire Safety J.*, **33**, 11–20.

Turner, J.S. (1973) *Buoyancy Effect in Fluids*, Cambridge University Press, UK.

Weng, W.G. and Fan, W.C. (2004) Nonlinear analysis of the backdraft phenomenon in room fires. *Fire Safety J.*, **39**, 447–464.

Weng, W.G., Fan, W.C., Yang, L.Z., Song, H., Deng, Z.H., Qin, J., and Liao, G.X. (2003) Experimental study of backdraft in a compartment with openings of different geometries. *Combust. Flame*, **132**, 709–714.

Yang, R., Weng, W.G., Fan, W.C., and Wang, Y.S. (2005) Subgrid scale laminar flamelet model for partially premixed combustion and its application to backdraft simulation. *Fire Safety J.*, **40**(2), 81–98.